Vehicle-to-grid optimization considering battery aging

N.B. When citing this work, cite the original published paper.

(article starts on next page)

Vehicle-to-Grid Optimization Considering Battery Aging

Chih Feng Lee *, **Kalle Bjurek** *, **Victor Hagman** **, **Yang Li** **,
Changfu Zou **

* *Polestar Performance AB, Gothenburg, Sweden.*
** *Chalmers University of Technology, Gothenburg, Sweden.*

Abstract: Electric vehicles (EVs) play a substantial role in reducing greenhouse gas emission and support a sustainable future. However, the increase of EV may lead to rising electricity demand and fluctuation. In this paper, the EV is proposed as a means to support the electricity grid via the vehicle-to-grid (V2G) technology. To reduce energy demand peaks, charging is planned during off-peak hours. Additionally, the EV battery may be used as a buffer to store energy during off-peak hours, and to supply energy to the grid during peak hours. Furthermore, grid frequency may be regulated by controlling the charging power. Since battery utilization will be increased during V2G operations, battery degradation is included in this study. A case study of Swedish households shows that the V2G is not only contributing to the stability of the grid, but may also help reducing the operating cost of an EV owner, even when battery degradation is considered.

1. INTRODUCTION

To curb climate change, the consensus is that fossil fuel-based electricity generation shall be replaced by renewable power generation, and combustion engine vehicles substituted by electric vehicles (EVs). However, due to the unpredictability of weather, an increased share of renewable power generation from weather-dependent sources reduces the production predictability. Furthermore, a higher market penetration of EVs imposes further challenges for the grid operators, particularly when a large number of EVs are charged simultaneously, creating peak power demand.

Recently, there are many proposed smart grid services for alleviating the conundrum of weather-dependent renewable power generation and rising EV share, namely the vehicle-to-home (V2H) and vehicle-to-grid (V2G), see (Thingvad and Marinelli, 2019; Bjurek and Hagman, 2022) and the references therein. In both applications, EV batteries are used to store electrical energy for later dispatch using a bidirectional charger. Specifically, V2H reduces peak power demand, while V2G strategies offer frequency regulation services to the transmission system operators (TSOs). By empowering EVs with smart grid technologies, the EV may become a part of the solution for stabilizing the grid, instead of being the cause of the problem.

However, as these services increase battery usage, there is a concern regarding premature battery degradation. As the lithium-ion battery is one of the most cost-intensive components in an EV, it is important to consider the degradation cost. Additionally, it is also imperative to prolong battery life to reduce the environmental impact, as the energy used for manufacturing new and decommissioning used-batteries is significant.

In this paper, V2G optimization problems with battery aging cost are investigated, where the contributions are threefold. Firstly, a linear battery aging model that captures incremental degradation during a V2G session is proposed. Secondly, the proposed model is utilized to formulate optimization problems for frequency balancing services using EVs. Finally, a case study in the Swedish market is analyzed and the results are discussed.

2. BATTERY ENERGY AND AGING MODEL

A battery pack consists of multiple cells connected both in series and parallel. In this paper, the characteristics of a 18650 Li-ion battery cell with carbon cathode and $Li(NiMnCo)O_2$ anode are used, where the specifications are given in Table 1. Furthermore, the pack consists of 10260 cells, where 95 strings are connected in parallel, and each string consists of 108 cells. Homogeneity of the cells is assumed.

Table 1. Battery cell specifications (Ecker et al., 2014; Schmalstieg et al., 2014).

Nom. Capacity	2.05 Ah	$\gamma_0 = 3.3324$	$\epsilon_0 = 7.543 \cdot 10^6$
Nom. Voltage	3.6 V	$\gamma_1 = 2.1021$	$\epsilon_1 = 23.75 \cdot 10^6$
Min. Voltage	2.5 V	$\gamma_2 = -5.8485$	$\epsilon_2 = 6976$
Max. Voltage	4.2 V	$\gamma_3 = 8.0326$	$\zeta_0 = 7.348 \cdot 10^{-3}$
Int. Resistance	0.0334 Ω	$\gamma_4 = -3.4599$	$\zeta_1 = 3.667$
			$\zeta_2 = 7.600 \cdot 10^{-4}$
			$\zeta_3 = 4.081 \cdot 10^{-3}$

2.1 Battery Energy Model

The battery model used for optimizing V2G operations shall capture the dynamics of battery SoC, as it dictates

how much energy can be charged or discharged from the battery. Another desirable model property is a fast computational speed. To this end, the energy reservoir model is adopted:

$$\frac{dz(t)}{dt} = \frac{P(t)}{b^{\text{cap,kWh}}}, \qquad z(t) \in [0, 1], \qquad (1)$$

where $z(t)$, $P(t)$, and $b^{\text{cap,Wh}}$ are respectively, the battery state-of-charge (SoC), power and pack energy capacity in kilowatt-hours.

Additionally, the battery open-circuit voltage, OCV can be fitted using

$$\text{OCV}(z) = \gamma_0 + \gamma_1 \cdot z + \gamma_2 \cdot z^2 + \gamma_3 \cdot z^3 + \gamma_4 \cdot z^4, \qquad (2)$$

where γ's are the polynomial coefficients listed in Table 1

2.2 Battery Aging Models

The battery capacity loss over time can be examined using the empirical degradation characteristic proposed in (Ecker et al., 2014; Schmalstieg et al., 2014). The model allows fitting to experimental data, which is favourable when the exact battery chemistry is not available. Furthermore, the model considers calendar aging and cycle aging individually. The total degradation is given by

$$C^{\text{lost}} = \alpha(V(t), \theta) \cdot T^{0.75} + \beta(V(t), z(t)) \cdot \sqrt{Q}, \qquad (3)$$

where $\alpha, \beta, \theta, V, T,$ and Q are respectively, the calendar aging factor, cycle aging factor, voltage, battery temperature, battery age in days, and the total energy throughput from the beginning-of-life in ampere-hours. Note that the latter two terms can be obtained from accelerated battery aging tests.

The calendar aging factor over a period, $\mathcal{T}$ is given by

$$\alpha(V, \theta) = (\epsilon_0 \cdot \bar{V} - \epsilon_1) \cdot \exp\left(-\frac{\epsilon_2}{\theta}\right), \qquad (4)$$

where $\bar{V}$ is the average voltage over the period, and ϵ_0 to ϵ_2 are the coefficients. Moreover, the cycle aging factor is

$$\beta(V, z) = \zeta_0 \cdot (\varnothing V - \zeta_1)^2 + \zeta_2 + \zeta_3 \cdot \Delta\text{DoD}, \qquad (5)$$

where $\varnothing V$ is the root-mean-square voltage, and ζ_0 to ζ_3 are the coefficients. The depth-of-discharge, ΔDoD is approximated as (Reniers et al., 2018),

$$\Delta\text{DoD} = \frac{2 \int |\bar{z} - z(t)| \, dt}{\mathcal{T}}, \qquad (6)$$

where $\bar{z}$ is the average SoC.

Incremental Aging Model. During V2G optimization, it is desirable to know the incremental degradation resulted from a chosen action during the control horizon. By utilizing Taylor series expansion, Bjurek and Hagman (2022) approximated of the incremental degradation over the control horizon, T^{hor} using

$$\tilde{C}^{\text{lost}} = 0.75 \cdot \alpha(V, \theta) \cdot \frac{T^{\text{hor}}}{T^{0.25}} + 0.5 \cdot \beta(V, z) \cdot \frac{Q^{\text{hor}}}{\sqrt{Q}}, \qquad (7)$$

where Q^{hor} is the energy throughput during the control time horizon. For ease of implementation, the T and Q prior to the control horizon are used when the control horizon is sufficiently short compared to the battery age. Furthermore, T^{hor} is typically given in a V2G optimization problem, and Q^{hor} is linear to battery power (the optimized variable) — allowing for linear problem formulation and may lead to faster optimization. The results from (3) and (7) are compared in Figure 1.
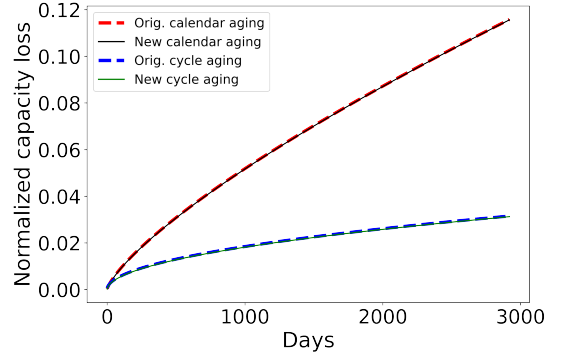

Fig. 1. Battery aging computed using the original (3) and the new model (7).

Linearized Incremental Aging Model. Note the incremental aging model (7) requires voltage as an input, which is dependent on the nonlinear OCV (2). To facilitate linear problem formulation, an affine voltage model is desirable. By assuming a small battery internal resistance, the voltage is close to the OCV. This assumption is typically acceptable as the battery internal resistive loss is relatively small compared to the energy transferred from/to the grid. Additionally, by assuming a sufficiently small SoC operating range over the investigated period, the mean voltage may be approximated using

$$\widehat{\overline{V}} = V^{\min} + \kappa \cdot \bar{z}, \qquad (8)$$

where $V^{\min}$ is the voltage at 0% SoC, $\bar{z}$ is the average SoC over the period, and κ is calculated using

$$\kappa = \frac{\Delta\text{OCV}}{\Delta z} = \frac{\text{OCV}(1) - \text{OCV}(0)}{1 - 0}.$$

By using the mean voltage, the linearized incremental aging model is then given by

$$\tilde{C}^{\text{lost,mv}} = \tilde{d}^{\text{cal}} + \tilde{d}^{\text{cyc}} \qquad (9a)$$

$$\tilde{d}^{\text{cal}} = 0.75 \cdot \alpha(\widehat{\overline{V}}, \theta) \cdot \frac{T^{\text{hor}}}{T^{0.25}} \qquad (9b)$$

$$\tilde{d}^{\text{cyc}} = 0.5 \cdot \beta(\hat{V}, \hat{z}) \cdot \frac{Q^{\text{hor}}}{\sqrt{Q}}, \qquad (9c)$$

where $\tilde{d}^{\text{cal}}$ and $\tilde{d}^{\text{cyc}}$ are the incremental capacity loss from calendar and cyclic aging, respectively. Further simplifications can be obtained if the following assumptions are made: The temperature, θ is assumed constant if the battery temperature is well controlled during V2G operation; A median voltage $\hat{V}$ for a typical cycle may be adopted if charge/discharge cycles are similar to each other in general; An appropriate $\hat{z}$ is chosen to approximate ΔDoD in the typical cycle.

Note that the proposed model (9) can be tuned for a given cyclic pattern to match (7). Therefore it provides improved flexibility compared to the fixed rate degradation model proposed by Reniers et al. (2018), where the lost capacity per cycle is given by

$$\tilde{C}^{\text{lost,fix}} = d^c \cdot \int |P(t)| dt, \qquad (10)$$

where $P(t)$ is the power trajectory during a cycle. Moreover, the degradation constant, d^c is determined by assum-

ing the battery reached its end-of-life (EoL)[1] after a predefined number of cycles. The fixed rate degradation model (10) cannot capture different degradation rates resulted from distinctive usage patterns.

3. VEHICLE-TO-GRID (V2G) OPTIMIZATION

In the following, an overview of the frequency regulation in electricity grid is first given, followed by the optimization problem formulation.

3.1 Overview of Frequency Regulation

For the electric power system to work efficiently, a balance between production and consumption of power is needed. A sudden deviation from the planned schedules of production and consumption will lead to a deviation of the grid frequency from the nominal, which is 50 Hz in Europe. A stable frequency is of utter importance since electrical appliances are constructed to work at a designated frequency, and a deviation can lead to non-working devices. Furthermore, large frequency deviations will cause instability problems, leading to failure in system operation. If the energy production is higher than consumption, the frequency of the grid will rise above the nominal value, and *down-regulation* of the frequency is necessary. On the other hand, if the consumption is higher than production, the frequency will drop under the nominal value, and *up-regulation* is required. Note the grid frequency is the same within a synchronous area, where the Nordic synchronous system covers Sweden, Finland, Norway, and the Eastern Denmark.

To maintain the frequency of the grid, Transmission System Operator (TSO) is appointed on a national or regional level. The TSO may offer remuneration for market participants who provide frequency regulation services. The rate of remuneration is dependent on the regulation product that is characterized by activation speed and endurance. In Sweden, the TSO is Svenska Kraftnät, and the products available are Fast Frequency Reserve (FFR), Frequency Containment Reserve (FCR), automatic Frequency Restoration Reserve (aFRR), and manual Frequency Restoration Reserve (mFRR) (Svenska Kraftnät, 2022). These products are traded on markets where participants can offer capacity of a product at a certain price, which can then be procured by the TSO. Furthermore, there are also requirements on the minimum bid size, i.e. the regulating capacity. While this might not be an issue for large market players, it prevents small-scale actors such as individual households from participating in frequency regulation markets. An approach to circumvent this issue is to aggregate the capacity of many smaller units such that the combined capacity can be traded. The market actor that consolidates capacity is called the aggregator. In the following, the Swedish frequency regulation services will be described.

Frequency Containment Reserve. The Frequency Containment Reserve (FCR) stabilizes the frequency in case of deviations and is a vital part of regulating the frequency

of the grid. The service is automatically activated if the frequency deviates inside the specified regulation region. The FCR is divided into two products, FCR-N where the letter N stands for normal operation, and FCR-D where the letter D stands for disturbed operation. Note that the product specifications and numbers in the following paragraphs are specific for the Swedish market (Svenska Kraftnät, 2022).

FCR-N is a frequency regulation product in both up and down directions. It is symmetrical as the offered capacity has to be available for activation in both directions. The region for activation is between 49.9 Hz to 50.1 Hz, and the minimum bid size is 0.1 MW. The approximate volume requirement for Sweden is 231 MW in 2023. The product is activated linearly, with 100% activation of the bid at 50.1 Hz and -100% activation at 49.9 Hz, where negative activation implies up-regulation. Regarding reaction time, 63% of the given activation must be made within 60 seconds of a deviation, and 100% within 3 minutes, while the activation endurance must be at least one hour.

Furthermore, FCR-D is a frequency regulation product offered in only one direction, and it is automatically activated to stabilize the frequency in the event of a disturbance when the frequency is outside the range of 49.9 Hz to 50.1 Hz. The FCR-D (up) focuses on up-regulation, where it is activated between 49.5 Hz to 49.9 Hz. The linear activation is adopted, with 100% activation if the frequency is at the lower end, 49.5 Hz and 0% activation if the frequency is at the higher end, 49.9 Hz. The minimum bid size is 0.1 MW and the volume requirement for Sweden is up to 558 MW in 2023. The required activation time is 50% within 5 seconds and 100% within 30 seconds, and endurance should be at least 20 minutes. Note that the FCR-D product portfolio was expanded in 2022 by introducing FCR-D (down) that focuses on down-regulation. In this paper, only FCR-D (up) will be considered since it is more applicable to the bidirectional charging use case.

Bidding Procedure and Remuneration. The FCR products can be procured in the one-day-ahead (D-1) or two-days-ahead (D-2) markets. These markets are closed one or two days before the actual delivery, where the deadline for submitting bids for D-1 is 18:00, and D-2 is 15:00. Note the majority of the capacity is procured in D-2. Additionally, the bids are held in closed auctions, so participants are unaware of each other's bids. When the bidding process ends, Svenska Kraftnät will consolidate the bids and sort them in ascending order, and then accept the bids with the lowest asking prices summing up to the total product volume requirement (Svenska Kraftnät, 2022).

Procured bids for FCR-N capacity are reimbursed according to "pay-as-bid". Additionally, the energy usage during activation is priced according to the up-regulation and down-regulation prices on Nord Pool power exchange.

On the other hand, the procured FCR-D bids are reimbursed according to "pay-as-bid", but there is no reimbursement or cost for activation.

3.2 Problem Formulation

FCR-N. The FCR-N bids are symmetrical in both up and down directions. During up-regulation, the EVs either

---

[1] The EoL for EV batteries is typically defined when 30% of the initial storage capacity is lost.

stop charging or enter discharge mode. Conversely, during down-regulation, the charging power is increased. The FCR-N problem with n_v vehicles, n_h households and over the next n_k hours is considered. Inspired by Dalton (2018), the problem is formulated as:

$$\min_{P_{k,i}^{\text{bat}}, P_k^{\text{bid}}} \quad \Pi^{\text{net}} - \Pi^{\text{bid,FCRN}} + \Pi^{\text{reg}} + \lambda^{\text{deg}} \tag{11a}$$

$$\text{s.t.} \quad \Pi^{\text{net}}$$
$$= \sum_{k=0}^{n_k} \left[\lambda_k^{\text{da}} \cdot \left(\sum_{h=1}^{n_h} E_{k,h} + \sum_{i=1}^{n_v} P_{k,i}^{\text{wall}} \cdot \Delta t \right) \right] \tag{11b}$$

$$\Pi^{\text{bid,FCRN}} = \sum_k \lambda_k^{\text{bid,FCRN}} \cdot P_k^{\text{bid}} \tag{11c}$$

$$\Pi^{\text{reg}} = \sum_k \lambda_k^{\text{reg}} \cdot R_k^{\text{D2C}} \cdot P_k^{\text{bid}} \tag{11d}$$

$$\begin{cases} z_{k+1,i} = \dfrac{P_{k,i}^{\text{bat}}}{b^{\text{cap,kWh}}} \cdot \Delta t + z_{k,i} \\ z^{\min} \leq z_{k,i} \leq z^{\max} \\ z_{0,i} = z_i^{\text{init}} \\ z_{n_k,i} \geq z^{\text{end}} \end{cases} \tag{11e}$$

$$\begin{cases} \lambda^{\text{deg}} = \sum_i \tilde{C}_i^{\text{lost,mv}} \cdot b^{\text{cost}} \\ \text{Equation (9)} \end{cases} \tag{11f}$$

$$\begin{cases} \sum_i P_{k,i}^{\text{wall}} \cdot \Delta t \geq -\sum_h E_{k,h} \\ P^{\min} \leq P_{k,i}^{\text{wall}} \leq P^{\max} \end{cases} \tag{11g}$$

$$\begin{cases} P_k^{\text{bid}} \leq \sum_i \left(P_{k,i}^{\text{wall}} + |P_i^{\min}| \right) \\ P_k^{\text{bid}} \leq \sum_i \left(P_i^{\max} - P_{k,i}^{\text{wall}} \right) \end{cases} \tag{11h}$$

$$P_{k,i}^{\text{wall}} + \frac{R_k^{\text{D2C}} \cdot P_k^{\text{bid}}}{n_v} = P_{k,i}^{\text{bat}} + (1-\eta) \cdot |P_{k,i}^{\text{bat}}| \tag{11i}$$

The objective function (11a) defines the total operating cost, which includes the net electricity costs for all households, Π^{net}, reimbursement from offered bids, Π^{bid}, cost/income from bought/sold energy during activation, Π^{reg}, and battery degradation cost, λ^{deg}. Without loss of generality, the sampling time, Δt is chosen as one hour, where the discrete time-step is $k = 0, 1, \ldots, n_k$.

The total household electricity cost (11b) is dependent on the day-ahead price, λ_k^{da}, household energy consumption, $E_{k,h}$, and the power exchanged between EV and wallbox, $P_{k,i}^{\text{wall}}$. Moreover, the bidding price, $\lambda_k^{\text{bid,FCRN}}$, regulation price, λ_k^{reg}, dispatch-to-contract ratio, R_k^{D2C}, day-ahead price and household energy consumption are assumed to be known *a priori*. The dispatch-to-contract ratio quantifies the proportion of the activated bids.

Furthermore, (11e) is the discretization of the battery energy model (1), where the permissible SoC range is defined in $[z^{\min}, z^{\max}]$, the initial SoC is given as z_i^{init}, and the final SoC constraint ensures the EV driver has at least the demanded SoC, z^{end} at the departure time.

As described in (11f), the battery degradation cost, λ^{deg} is a product of the lost battery capacity, $\tilde{C}_i^{\text{lost,mv}}$ and the cost of a new battery b^{cost}, where the lost battery capacity is modeled using (9).

Additionally, the wallbox power constraint (11g) restricts the total energy discharged from all EVs to be at most

the total household energy consumption. Therefore, the same total energy is drawn from the grid across different solutions. Moreover, the wallbox has hardware limitations, where the power is restricted within $[P^{\min}, P^{\max}]$.

The bid size is constrained by (11h), where the maximum up-regulation bid is limited by the sum of the actual charging power and the maximum discharging power. Similarly, the maximum down-regulation bid is bounded by the difference between the maximum and actual charging power.

Finally, (11i) expresses the relationship between wallbox power and battery power, where the charging/discharging efficiency, $\eta \in (0,1)$, and the activation of offered bid are considered. The power from activating the bids is assumed to be equally distributed over all EVs.

FCR-D (up). The FCR-D (up) optimization problem is defined as:

$$\min_{P_{k,i}^{\text{bat}}, P_k^{\text{bid}}} \quad \Pi^{\text{net}} - \Pi^{\text{bid,FCRD}} + \lambda^{\text{deg}} \tag{12a}$$

$$\text{s.t.} \quad \text{Equations (11b), (11e)--(11g)}$$

$$\Pi^{\text{bid,FCRD}} = \sum_k \lambda_k^{\text{bid,FCRD}} \cdot P_k^{\text{bid}} \tag{12b}$$

$$P_k^{\text{bid}} \leq \sum_i \left(P_{k,i}^{\text{wall}} + |P_i^{\min}| \right) \tag{12c}$$

$$P_{k,i}^{\text{wall}} = P_{k,i}^{\text{bat}} + (1-\eta) \cdot |P_{k,i}^{\text{bat}}| \tag{12d}$$

The total cost of operation for FCR-D (up) (12a) consists of the net household electricity cost, the revenue from offering the bids, and the cost of battery degradation.

Moreover, expressions for the total household electricity cost, battery energy model, wallbox power constraint and battery degradation cost are shared with the FCR-N problem formulation defined in (11). Furthermore, the FCR-D revenue can be calculated using the bid price, $\lambda_k^{\text{b,FCRD}}$. Note the regulation bid only has one constraint, depicting the case where EVs stop charging and discharge at the maximum rate, as defined in (12c). Additionally, the power transfer efficiency between EV and wallbox is considered in (12d). However, no activation of the offered FCR-D (up) bids is being considered in this study, as it is a relatively rare occurrence.

Note that the optimization problems (11) and (12) consist of absolute value functions that are not differentiable, but can be transformed to standard linear program forms using standard techniques found in (Boyd et al., 2004, p. 6). Additionally, the problems are modeled using Pyomo (Bynum et al., 2021; Hart et al., 2011), and solved using the linear programming toolbox, Gurobi (Gurobi Optimization, LLC, 2022).

4. CASE STUDY OF SWEDISH HOUSEHOLDS

4.1 Assumptions

To investigate the potential saving by using V2G services, a large fleet of vehicles with randomized driving behavior was simulated, where the average driving distance per day, battery age, and the arrival SoC for each EV were sampled from truncated Gaussian distributions defined in Table 2.

The mean daily travel distance are chosen according to the Swedish data in 2021 (Trafikanalys, 2021). The end SoC was set to be at least 70%, for all EVs.

Table 2. Truncated Gaussian distribution parameters.

	Mean	SD	Min	Max
Daily Travel [km]	30	20	5	100
Battery Age [day]	365	365	30	1095
Arrival SoC [%]	45	10	35	55

Additionally, the seasonal effect was investigated on the four days listed in Table 3. The days were arbitrarily chosen but spread evenly throughout a year.

Table 3. Days used for the case study.

	Arrival Time	Departure Time
Day 1 (Summer)	2021-07-11, 17:00	2021-07-12, 08:00
Day 2 (Autumn)	2021-10-11, 17:00	2021-10-12, 08:00
Day 3 (Winter)	2022-01-11, 17:00	2022-01-12, 08:00
Day 4 (Spring)	2022-04-11, 17:00	2022-04-12, 08:00

Furthermore, the vehicles are assumed to be plugged-in overnight from 5 pm to 8 am on the selected days. As the actual value of dispatch-to-contract ratio, R_k^{D2C} was not easily accessible, an estimation was deduced from the historical data from the Nordic Synchronous System using

$$R_k^{\text{D2C}} = \begin{cases} \max\left(\frac{f_k - 50.0}{50.00 - 49.90}, -1\right), & \text{if } f_k < 50.00 \\ \min\left(\frac{f_k - 50.0}{50.00 - 49.90}, 1\right), & \text{if } f_k \geq 50.00, \end{cases} \quad (13)$$

where f_k is the frequency with the maximum deviation from 50.00 Hz within the k-th hour. The frequency data was obtained from Fingrid (2022), which had a resolution of three minutes. By selecting the frequency with the maximum deviation from 50.00 Hz within each hour, the worst-case activation was achieved. The resulting activation profiles for the chosen days are shown in Figure 2. Note that a negative activation implies that the frequency was lower than 50.00 Hz.
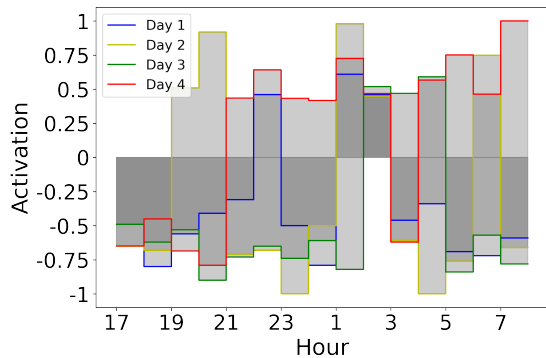

Fig. 2. FCR-N activation for Days 1 to 4.

4.2 Results and Discussions

The total electricity consumption cost for a fleet size of 1000 EVs and 1000 households are shown in Table 4, where Smart Charging (SC), V2H-G, FCR-N and FCR-D are investigated. SC represents the baseline use case, where a
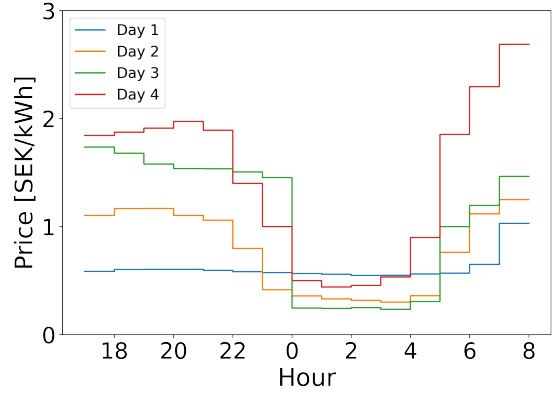

Fig. 3. Hourly electricity price for Days 1 to 4.

Table 4. Electricity and battery degradation costs, and the potential savings with V2H/V2G services.

		Direct [SEK]	Cyc. [SEK]	Cal. [SEK]	Total [SEK]	Savings [%]
Day 1	SC	19,202	4,020	3,348	26,571	-
	V2H-G	18,911	4,115	3,334	26,359	0.8
	FCR-N	-28,301	5,341	3,618	-19,342	172.8
	FCR-D	-59,027	4,116	3,334	-51,578	294.1
Day 2	SC	25,588	4,020	3,342	32,950	-
	V2H-G	15,606	6,609	3,208	25,424	22.8
	FCR-N	-55,721	11,363	2,929	-41,429	225.7
	FCR-D	-78,792	7,188	3,310	-68,294	307.3
Day 3	SC	47,504	4,020	3,378	54,902	-
	V2H-G	16,711	11,012	3,035	30,758	44.0
	FCR-N	-32,693	9,149	2,937	-20,608	137.6
	FCR-D	-55,228	11,211	3,041	-40,976	174.6
Day 4	SC	52,679	4,020	3,421	60,120	-
	V2H-G	27,620	8,698	3,139	39,457	34.4
	FCR-N	-6,116	10,830	2,796	7,510	87.5
	FCR-D	-24,050	8,590	3,163	-12,297	120.5

cost-minimizing EV charging schedule is adopted without discharging the battery to feed the grid. V2H-G represents V2H with the possibility of feeding energy to the grid. Even though the problem formulations for SC and V2H-G are not discussed in this paper, the results are included here for completeness. For details please refer to (Bjurek and Hagman, 2022).

A close inspection of Day 1 reveals that V2H-G marginally improves the saving compared to SC. This is due to a combination of very low variance in electricity price within the optimization horizon (see Figure 3), and a relatively low household energy consumption (see Figure 4). The cycle aging cost is higher than the fluctuations found in electricity price (except for 7 am). Between 7 am and 8 am, the EVs are discharged to the households, yielding the observed marginal saving. On the other investigated days, V2H-G improves the baseline cost saving of up to 44% due to the higher consumptions and price fluctuations.

FCR-N shows a great cost reduction potential because of the revenue received from frequency regulation. For the three out of four investigated days, the total costs are negative, implying the household owners obtain a profit, as the revenue from frequency regulation bids is greater than the total cost for energy consumption and battery degradation. However, note that the adopted assumptions about *a priori* knowledge of activation and the hourly

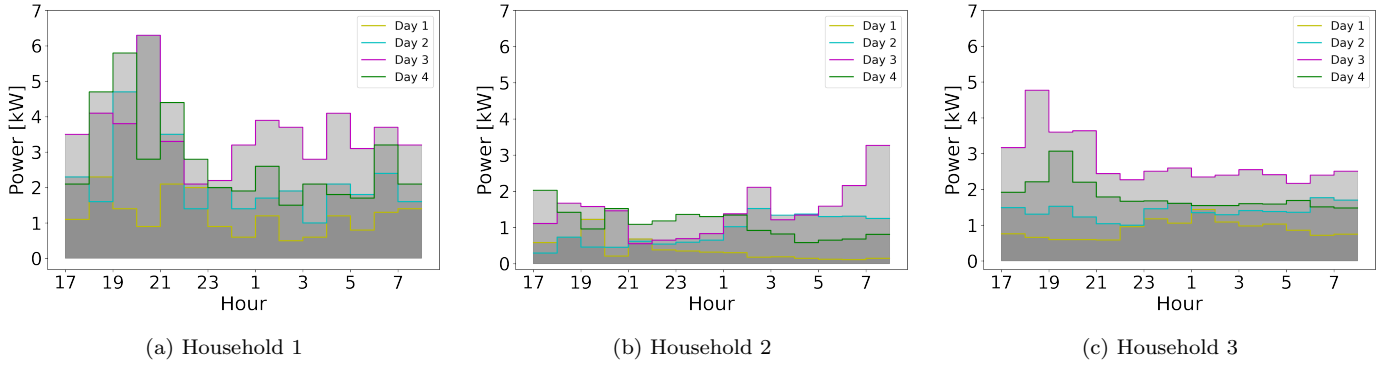(a) Household 1   (b) Household 2   (c) Household 3

Fig. 4. Household energy consumption for Days 1 to 4.

dispatch-to-contract ratio are simplification of the real-world conditions, which may result in an optimistic result. Nevertheless, this encouraging result motivates further investigations. For practical implementation, the lack of knowledge about future activation can be tackled using a conservative approach, for example, by offering FCR-N only using unidirectional charging, i.e., stop charging or charge more than planned, as this would not risk depleting the batteries and reducing the degradation cost.

Furthermore, FCR-D (up) yields the lowest total cost and shows good profits. Since the activation of FCR-D (up) is typically rare, the charging behavior is minimally affected. Note that for the three out of four days, the cycle aging costs are higher than V2H-G. This is not expected intuitively, as no activation is triggered. A careful investigation reveals that this is caused by the higher bid offering remuneration compared to the sum of day-ahead electricity price and cycle aging marginal cost — the EVs are actually charged more than necessary to be able to offer a larger bid. For example, on Day 2, the EVs reached an average final SoC of 76%, compared with the lower limit of 70%. On Day 3, the EV fleet is charged with a slightly higher power during 8 pm in order to increase the bid for that specific hour. As a result, the EVs are then able to discharge more energy to the households at 5 am on the following day, when the bid offering remuneration is lower. The charging-discharging leads to a higher battery throughput and cycle aging cost. The calendar aging is also increased due to the increased average SoC.

5. CONCLUDING REMARKS

A linearized battery model and problem formulation are utilized to study the V2G with aggregated fleet of EVs, where battery degradation cost is considered. By investigating the V2G cases involving three Swedish household consumptions in various seasonal conditions, the FCR-D (up) is emerged as the most profitable frequency balancing product offer, with the lowest entry requirement.

To improve the representation of battery dynamics during optimization, a nonlinear, nonhomogeneous battery pack model with thermal effects may be considered in future work.

REFERENCES

Bjurek, K. and Hagman, V. (2022). *Vehicle-to-Everything Optimization Considering Battery Degradation*. Mas-ter's thesis, Chalmers University of Technology.

Boyd, S., Boyd, S.P., and Vandenberghe, L. (2004). *Convex optimization*. Cambridge University Press.

Bynum, M.L., Hackebeil, G.A., Hart, W.E., Laird, C.D., Nicholson, B.L., Siirola, J.D., Watson, J.P., and Woodruff, D.L. (2021). *Pyomo–optimization modeling in python*, volume 67. Springer Science & Business Media, third edition.

Dalton, J. (2018). *Optimal Day-Ahead Scheduling and Bidding Strategy of Risk-Averse Electric Vehicle Aggregator: A Case Study of the Nordic Energy and Frequency Containment Reserve Markets*. Master's thesis.

Ecker, M., Nieto, N., Käbitz, S., Schmalstieg, J., Blanke, H., Warnecke, A., and Sauer, D.U. (2014). Calendar and cycle life study of Li(NiMnCo)O2-based 18650 lithium-ion batteries. *Journal of Power Sources*, 248, 839–851.

Fingrid (2022). Download datasets. URL https://data.fingrid.fi/open-data-forms/search/en/.

Gurobi Optimization, LLC (2022). Gurobi Optimizer Reference Manual. URL https://www.gurobi.com.

Hart, W.E., Watson, J.P., and Woodruff, D.L. (2011). Pyomo: modeling and solving mathematical programs in Python. *Mathematical Programming Computation*, 3(3), 219–260.

Reniers, J.M., Mulder, G., Ober-Blöbaum, S., and Howey, D.A. (2018). Improving optimal control of grid-connected lithium-ion batteries through more accurate battery and degradation modelling. *Journal of Power Sources*, 379, 91–102.

Schmalstieg, J., Käbitz, S., Ecker, M., and Sauer, D.U. (2014). A holistic aging model for Li(NiMnCo)O2 based 18650 lithium-ion batteries. *Journal of Power Sources*, 257, 325–334.

Svenska Kraftnät (2022). Svenska kraftnät. URL https://www.svk.se/.

Thingvad, A. and Marinelli, M. (2019). Influence of V2G Frequency Services and Driving on Electric Vehicles Battery Degradation in the Nordic Countries. In *Proceedings of the 31st International Electric Vehicles Symposium & Exhibition (EVS31) & International Electric Vehicle Technology Conference 2018 (EVTeC 2018)*.

Trafikanalys (2021). Körsträckor 2021. URL https://www.trafa.se/globalassets/statistik/vagtrafik/korstrackor/2021/korstrackor-2021.pdf.